Pressure-induced radial collapse in few-wall carbon nanotubes: A combined theoretical and experimental study

R. S. Alencar[a,b], Wenwen Cui[a], A. C. Torres-Dias[a,b], Tiago F. T. Cerqueira[a,c], Silvana Botti[c,a,d], Miguel A. L. Marques[e,a,d], O. P. Ferreira[b], Ch. Laurent[f], A. Weibel[f], D. Machon[a], D.J. Dunstan[g], A. G. Souza Filho[b], A. San-Miguel*[a]

[a] *Univ Lyon, Université Claude Bernard Lyon 1, CNRS, Institut Lumière Matière, F-69622 LYON, France*
[b] *Departamento de Física, Universidade Federal do Ceará, Fortaleza, Ceará, 60455-900 Brazil*
[c] *Institut für Festköpertheorie und -optik, Friedrich-Schiller Universität Jena, Max-Wien Platz 1, 07743 Jena, Germany*
[d] *European Theoretical Spectroscopy Facility*
[e] *Institut für Physik Martin-Luther-Universität Halle-Wittenberg, D–06099 Halle, Germany*
[f] *CIRIMAT, Université de Toulouse, CNRS, INPT, UPS, Toulouse, France*
[g] *School of Physics and Astronomy, Queen Mary University of London, London E1 4NS, UK*

Abstract

We study the pressure induced collapse of single-, double- and triple-wall carbon nanotubes. Theoretical simulations were performed using density-functional tight-binding theory. For tube walls separated by the graphitic distance, we show that the radial collapse pressure, P_c, is mainly determined by the diameter of the innermost tube, d_{in} and that its value significantly deviates from the usual $P_c \propto d_{\text{in}}^{-3}$ Lévy-Carrier law. A modified expression,

*Corresponding author. E-mail: alfonso.san-miguel@univ-lyon1.fr

$P_c d_{\rm in}^{-3} = \alpha(1 - \beta^2/d_{\rm in}^2)$ with α and β numerical parameters, which reduces the collapse pressure for low diameters is proposed. For $d_{\rm in} \gtrsim 1.5$ nm an enhanced stability is found which may be assigned as due to the bundle intertube geometry-induced interactions. If the inner and outer tubes are separated by larger distances, the collapse process is found to be more complex. High-pressure resonant Raman experiments were performed in double-wall carbon nanotubes having inner and outer diameters averaging 1.5 nm and 2.0 nm, respectively. A modification in the response of the G-band and the disappearance of the radial breathing modes between 2 GPa and 5 GPa indicate the beginning and the end of the radial collapse process. Experimental results are in good agreement with our theoretical predictions, but do not allow to discriminate from those corresponding to a continuum mechanics model.

1. Introduction

Carbon nanotubes (CNTs) are nanostructures composed by one or by multiple concentrically aligned cylindrical shells (walls) of carbon atoms. They have excellent mechanical resilience, due to the specific geometrical arrangement of carbon atoms and to the unique strength of the carbon-carbon bond. Furthermore, CNTs can be either semiconducting or metallic, depending on their chirality. Such remarkable properties triggered an ever increasing number of studies on their applicability for engineering nanodevices, reinforced composites, biomedical usage, among other applications [1].

While CNTs possess Young moduli along their symmetry axis in the terapascal range [2, 3], pressures in the gigapascal domain are enough to deform their radial cross-section [4]. Upon application of pressure, the radial cross-section evolves towards a collapsed conformation, often described as peanut-shaped. The transition towards this ultimate cross-section defines the geometrical collapse of a CNT [5, 6]. Since radially deformed CNTs present different and even possibly enhanced electronic [7] and mechanical properties [8], understanding the radial deformation and the collapse process can offer new opportunities for engineering devices and composites [9].

Theoretical studies have proposed a collapse of single-wall CNTs following a Lévy-Carrier type law [10–12], $P_{\mathrm{c}} \propto d^{-3}$, where P_{c} is the collapse pressure and d is the tube diameter [13]. This result corresponds to a continuum medium theory in which the proportionally constant includes the bending rigidity D of the considered material. Recent Raman experiments at high pressure [14] are consistent with this theoretical calculations. Furthermore, it is known that filling single-wall CNTs with different molecules, including even other CNT, can alter their mechanical stability [14–20]. More precisely, it has been proposed that homogeneous filling leads to an increase of the collapse pressure [17], and the effect is known to be particularly strong for water filling of single-wall nanotubes [14]. Environment [21–24] and bundling [25, 26] have also been proposed to influence the CNT's radial stability against pressure. We note that many of these effects are difficult to control in experiments, being probably the major reason for discrepancies between theory and exper-

iments. In addition, many experimental high-pressure studies performed on CNT's are based on resonant Raman spectroscopy, which requires the careful consideration of the evolution with pressure of the resonance conditions [27–29]. Finally we can also underline that deviations from the Lévy-Carrier scheme have been also proposed [6, 30] which will be discussed later.

A double-wall CNT can be viewed as a single-wall tube filled by another single-wall tube. As such, and in view of the above, it is reasonable to expect that the inner tube provides mechanical support, while the outer tube screens the environment [17, 31, 32]. Therefore, double-wall tubes are believed to show higher mechanical stability than single-wall CNTs. Unfortunately, it is difficult to extract from the different experimental and theoretical works published up to now a coherent picture on the collapse of CNTs having more than one wall.

Some theoretical results indicate that P_{c} in double-wall CNTs depends mainly on the diameter of the inner tube d_{in} [33]. In contrast, other studies obtain that P_{c} is a function of the average of d_{in} and d_{out}, respectively the inner and outer tube diameters [34]. This result implies that not only d_{in}, but also the distance between the walls, are relevant factors in the collapse process. By averaging over samples having d_{in} varying from 0.5 to 1.9 nm, some experimental studies proposed that geometrical changes happen already at pressures as low as 3 GPa [35], and the response is elastic up to pressure of at least 10 GPa [36]. Other dynamic high-pressure experiments found that only minor tube structure damage occurs below 19 GPa, with the collapse of the

double-wall CNT occurring at $\sim$ 26 GPa [37]. However, other works which considered similar diameter distributions reported collapse or large structural modifications at different pressures ranging from $\sim$ 13–15 GPa [18, 38] to $\sim$ 25 GPa [17, 39]. Such important discrepancies can be attributed to the difficulty in working with double-wall CNT samples, mainly due to the large diameter distribution, the effect of the environment on the resonance conditions, and the presence of defects, which depend on synthesis, preparation and handling of the samples.

In this work we shed some light on this problem by performing systematic simulations of a large number of few-wall (1, 2, and 3 walls) CNTs, including tubes having different inter-wall separation. These simulations are performed using density-functional tight-binding theory (DFTB) [40], that provides an excellent compromise between accuracy and numerical efficiency for carbon-based systems. We also perform an experimental study of the mechanical response and collapse of double-wall CNTs as a function of pressure for samples having inner and outer diameter distributions larger than those previously reported.

2. Methodology

2.1. Theoretical methods

Density functional tight-binding [40] calculations were performed using the DFTB+ software package [41] with the matsci-0-3 parameter set [42]. This approach can be seen as an approximation to the Kohn-Sham density-functional theory, where the usual integrals are fitted to reference calcula-

tions. This allows for faster simulations, while keeping much better transferability and accuracy than other semi-empirical methods. This method is particularly good for carbon compounds as demonstrated in previous works [18, 43–45]. In particular, the carbon-carbon Slater-Koster parameters implemented in our work have been extensively used in the study of CNTs since at least 2003 [46]. We recently used these parameters to study the collapse of bundles of single-wall CNTs [13, 30]. Since carbon nanotubes are relatively inert structures where no significant charge transfer is expected [43], we decided to adopt the non-self-consistent charge scheme of DFTB.

Hexagonal unit cells containing two nanotubes with periodic boundary conditions in the three directions were used for a better description of the bundle geometry [13]. To keep calculations feasible, we chose only armchair nanotubes with diameters ranging from 0.6 nm to 3.3 nm: 24 single wall, 22 double wall and 5 triple wall (results for single-wall CNTs with diameter below 1.9 nm were taken from Ref. [13]). Triple-wall nanotubes with inner diameters larger than $\sim$1.2 nm were unfortunately too large to be handled in this work. The initial intra-tube distance of the multi-walled CNTs is fixed by the choice of the diameters of the inner and outer tubes. We first selected inner and outer tubes compatible with available experimental data, then we varied the diameters in two different ways: (i) maintaining as much as possible constant the intra-tube distance (with a reference value of about 0.335 nm); (ii) increasing the diameter of the external tube, while keeping fixed the diameter of the internal tube, and therefore increasing the

intra-tube distance. Quasi-static simulations were performed as follows: For each value of pressure, a random displacement of 0.002 nm, was applied on each atom in order to break all symmetries. Atomic positions and cell vectors were optimized until the magnitude of all forces became smaller than 10^{-4} Ha/Bohr. The applied pressure was increased in steps of 0.2 GPa up to 30 GPa or until collapse. The collapse of the tubes is abrupt in the large majority of the cases and was identified by a discontinuity in the enthalpy, that corresponds to the transformation to a peanut-like geometry. In some rare cases, especially at low diameters, this discontinuity was not found and the collapse pressure was determined by inspection, i.e., we assigned the collapse to the first peanut-like geometry found. According to this method the obtained collapse pressure corresponds to the end of the collapse process.

Impurities or defects, as well as the bundle size could also affect the collapse process. Its study is nevertheless not feasible using our quantum mechanical theoretical methods. In fact, the periodicity imposed by the DFTB calculations would imply to use a supercell containing a full bundle with a pressure transmitting medium, making the calculation too heavy.

2.2. Experimental setup and sample characterization

Samples were prepared by catalytic chemical vapor deposition. A detailed description of the synthesis methodology can be found in Ref. [47]. HRTEM Histograms were obtained (see supplementary material) showing the distribution of the number of walls and diameters for the double-wall CNTs studied in this work. A large majority of the tubes (80%) has been

observed with an average diameter of 1.5 nm and 2.0 nm for the inner and outer tubes, respectively. Therefore, the signal originated from these tubes is expected to dominate the resonant Raman spectra [47].

High pressure experiments were carried out using a diamond anvil-cell device, with low-fluorescence diamond anvils, having culet sizes of 600 μm. The sample was loaded in a cylindrical pressure chamber with a diameter of 250 μm and thickness of $\sim$90 μm drilled in a pre-indented stainless steel gasket. In-situ Raman measurements were performed using an Acton 300i system, with the excitation energy provided by a 2.41 eV (514.5 nm) laser, having the output power controlled to avoid temperature effects. NaCl was used as pressure transmitting medium to avoid any accidental filling of the tubes [14]. A small ruby chip was loaded with the sample to calibrate the pressure by using the standard ruby luminescence R1 line [48].

3. Results and discussion

3.1. Numerical simulations

To clarify the role of the diameter on the collapse in few-walled CNTs we performed DFTB [40] calculations for a selection of armchair (n, n) CNTs. Figure 1 shows the calculated normalized collapse pressures, as function of the inner tube diameter, for the single-wall (green triangles), double-wall (blue circles), and triple-wall (red squares) CNTs. This normalized collapse pressure, P_N, is defined as $P_N = P_c d_{in}^3$ and allows then to better observe deviations from the Lévy-Carrier law which in then represented by a horizontal line. As discussed above, our calculated values correspond to the end

of the tube collapse process. Figure 1 puts into evidence deviations from the Lévy-Carrier behavior in practically all the domain of explored diameters. We can nevertheless distinguish two clearly different regions. First of all we consider the region for $d_{\rm in} \lesssim 1.5$ nm. In this region the collapse pressure appears to evolve with independence of the number of tube walls and can be fitted with a same model already proposed for SWCNT [30]:

$$P_{\rm N} = P_{\rm c} d_{\rm in}^3 = \alpha \left(1 - \frac{\beta^2}{d_{\rm in}^2}\right) \quad \text{GPa nm}^3\,, \tag{1}$$

This modified Lévy-Carrier model corrects the observed deviations from continuum mechanics predictions by introducing a parameter $\beta \neq 0$ which accounts for the discretization of compliances for low tube diameters [30]. The value of β can be also interpreted as the lowest diameter self-sustained stable carbon nanotube which of course has no lower limit in a continuum medium theory. The value of α on its side is related to the bending rigidity, D, of the tube material in the continuum mechanics model and to the one of a graphene foil for SWCNT [30]. We obtain when fitting altogether the data of one- two- and three-walled tubes values of $\alpha = 13.8 \pm 1.2$ GPa nm^3 and $\beta = 0.48 \pm 0.03$ nm. The obtained value of β is in very good agreement with the published result for SWCNT on individualized tubes $\beta = 0.44 \pm 0.04$ nm obtained combining experiments and models [30]. Recalling that $\alpha = 24D$ [30], the obtained α value could be then associated to the bending rigidity D of the tube wall. We may then try to fit separately the data for one- two- and three-wall tubes respectively to obtain the associated bending

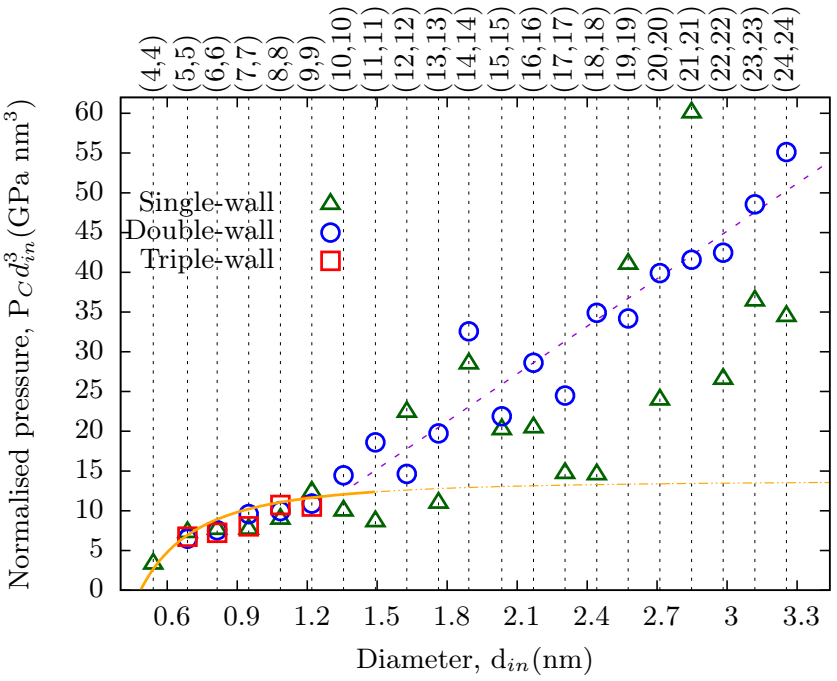

Figure 1: Calculated normalized collapse pressure as a function of the diameter (SWCNT) or inner diameter (for double and triple-wall tubes) of bundled few-wall CNTs. The internal diameter has been changed while keeping the intra-layer distance constant (or as close as possible, see text). All tubes are armchair, i.e.(n,n). The corresponding (n,n) indexes for the innermost tube is given in the upper scale. The continuous line corresponds to the fit using the modified Lévy-Carrier formula in Eq. 1 on the calculated data up to $\sim$ 1.5 nm. The dotted line is its extrapolation for larger diameters. The dashed line (in blue) is the linear fit to the deviations from the Lévy-Carrier formula for the double-wall tubes data given by $P_N = a + bd_{in}$ with $a = -15 \pm 5$ GPa nm^3 and $b = 20 \pm 2$ GPa nm^2.

rigidity in each case. Unfortunately we obtain in that case D values of 2.1, 2.5 and 2.1 eV, which do not correspond to a logical progression. We then prefer just to consider here the average value of α which significance is just a fitting parameter, probably affected by the more complex collapse process in carbon nanotubes having more than one wall.

We may consider now the second region in Figure 1 corresponding to internal tube diameters beyond $\sim$ 1.5 nm. In this regions deviations from the extrapolated curve from Eq. 1 become very significant. Even if there is a strong scattering in the calculated values, they increasingly differ to the expected extrapolation of the the values given by Eq. 1 (discontinuous line in Fig. 1) which in that region correspond well to the Lévy-Carrier expectations. These deviations appear to be linear with pressure in the case of DWCNT but are much more scattered for SWCNT. To explain such deviation, there is a need for a stabilizing contribution which is not included in a continuum medium model or even in Eq. 1 - which only corrects that model for low diameter tubes. The collapse process involves the modification of the tube curvature leading in the case of an isolated tube to a transition structure having important regions with zero curvature [49]. In the case of carbon nanotube bundles, the hexagonal symmetry can lead to the observation of tube hexagonalized cross-section due to pressure application as it has been proposed from neutron diffraction experiments [50] and to geometrical constraints leading to zig-zag orientation of the tubes at the collapse as it has been seen in DFTB calculations [13]. In fact, as it is shown in Fig. 2 we do

observe such polygonization even for internal tube diameters of 1.1 nm in both double-wall or triple-wall tubes.

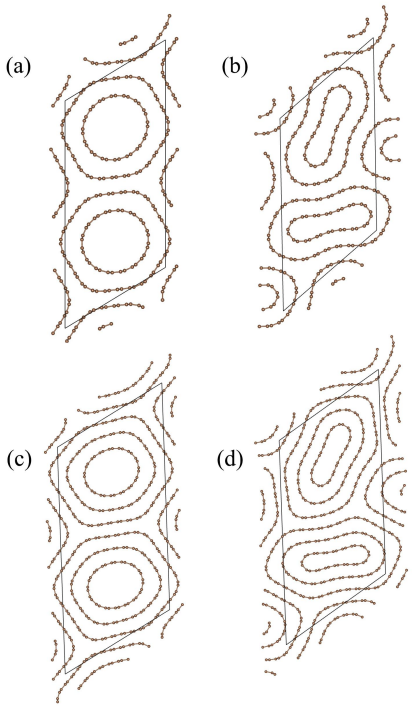

Figure 2: Snapshots before and after collapse. (a) and (b) are for (8,8)@(13,13) tubes. (c) and (d) are the (8,8)@(13,13)@(18,18) before and after collapse, respectively. The polygonization of the structure before the collapse can be clearly appreciated.

In Fig. 3a we show the collapse process as a function of the number of walls for the case of a $(8, 8)$ single-wall tube (green curve), a $(8, 8)@(13, 13)$ double-wall tube (blue curve), and a $(8, 8)@(13, 13)@(18, 18)$ triple-wall tube (red curve). For single-wall CNTs our calculations show a collapse transition usually quite abrupt [13], with a sharp transition to a peanut shape following a (small) compression of the tube. For double- and triple-walls there is a greater reduction of the volume before the collapse (see Fig. 3a), with the

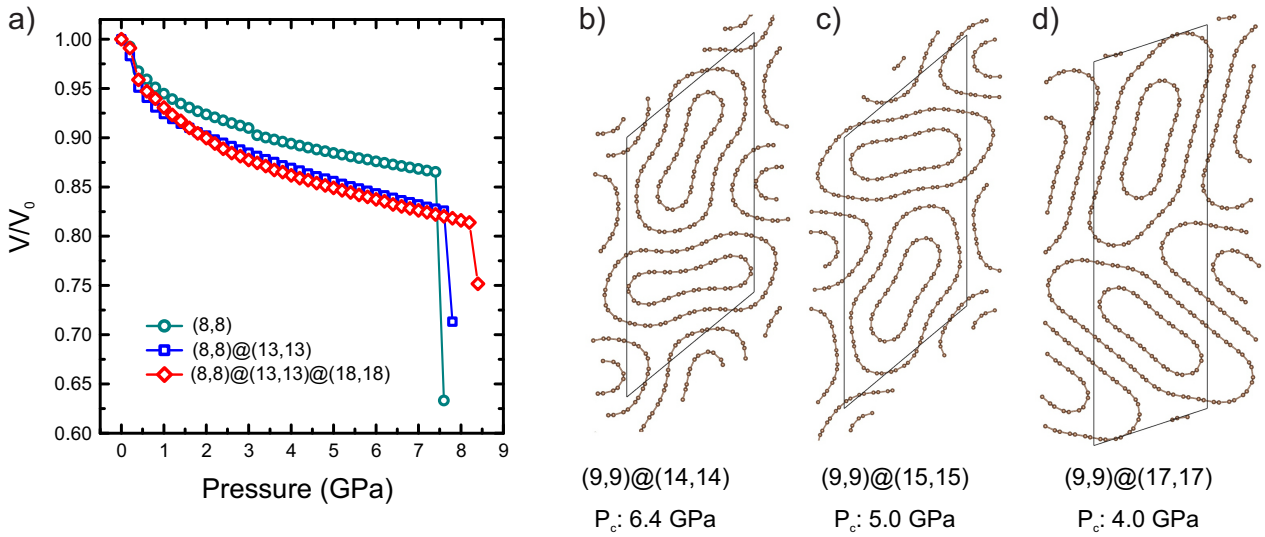

Figure 3: (a) Collapse pressure as function of the number of walls. DFTB calculated volume variation up to the onset of the collapse for $(8,8)$ single-wall tube (green curve), a $(8,8)$@$(13,13)$ double-wall tube (blue curve), and a $(8,8)$@$(13,13)$@$(18,18)$ triple-wall tube (red curve). (b)-(d) Collapse pressure as function of the tube-tube interwall distance. Calculated collapsed configurations and respective collapse pressures (labeled at the bottom) of double-wall tubes having a (9,9) inner tube, but three different larger outer tubes.

outer (larger) tube starting to deform at lower pressures, but being supported by the innermost (smaller) tube (see Fig. 2). The cross-section modification of the outermost tube causes an inhomogeneous strain on the innermost tube, which can then favor the collapse process with respect to the single-wall nanotube case.

Finally, we investigated the collapse of a double-wall CNT as a function of the distance between the inner and the outer tube. We chose as the inner tube a $(9, 9)$ CNT with a diameter of 1.22 nm, and for the outer tubes a $(14, 14)$, a $(15, 15)$, and a $(17, 17)$ CNT, leading to a inter-tube spacing of 0.34, 0.41, and 0.54 nm. The calculated collapse pressures for the three cases were 6.4, 5.0, and 4.0 GPa respectively, and the geometry of the collapsed tubes are depicted in Figs. 3b-d. As we can see, there is a considerable decrease of the collapse pressure with increasing inter-wall separation. This observation can again be explained by the larger ovalization of the outer tube, leading to an inhomogeneous compression of the inner tube favoring collapse.

The different elements arising from the discussion of Fig. 3 illustrate a more complicate image of the tube collapse process when increasing the number of walls which justifies then that the α parameter in Eq. 1 deviates from a simple association to a tube bending rigidity interpretation.

3.2. Experimental characterization

Details of the Raman spectra data analysis are provided in the Supplementary information. Figure 4a shows the DWCNTs Raman spectra of the

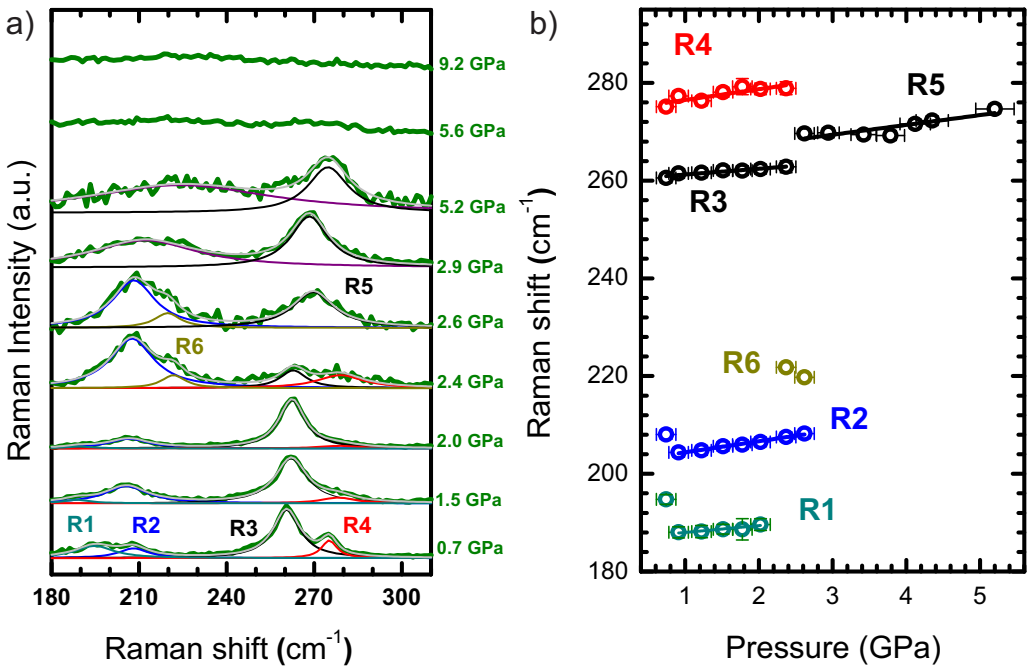

Figure 4: (a) RBLM Raman spectra collected at different pressures. Green and gray colors indicate data and fitting, respectively. Violet indicates a non-RBLM feature centered at $\sim$ 210 cm^{-1}. The remaining colors highlight the labeled RBLM features. (b) RBLM Raman frequencies of the six peaks shown in (a) as a function of pressure.

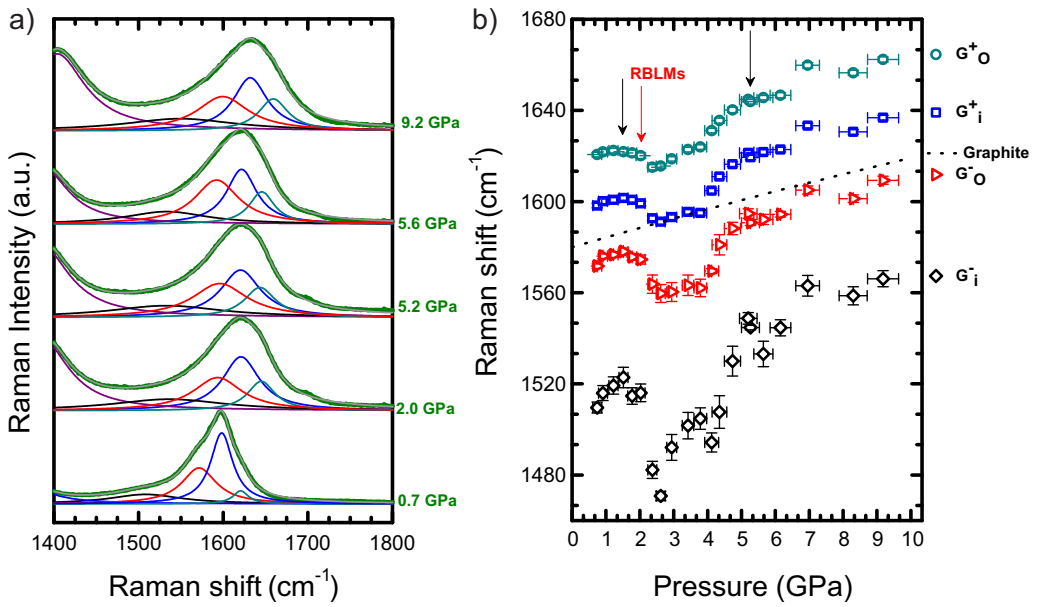

Figure 5: (a) G-band Raman spectra collected at different pressures. Green and gray colors indicate data and fitting, respectively. Violet indicates an overlap of the signal from diamond and the pressure transmitting medium at $\sim$ 1300-1400 cm^{-1}. The remaining colors highlight the G-band components. (b) Raman frequencies of the G-band components as function of pressure. The color code is the same used in panel (a). The two black arrows at $\sim$1 and $\sim$ 5 GPa indicate the beginning and the end of the collapse process as observed from the G-band signal. The red arrow labeled "RBLMs" points to the pressure at which total attenuation of the RBLM is observed. The pressure dependence of the G-band of graphite (dashed black line) is included for comparison.

radial breathing like modes (RBLMs) for a pressure ramp from 0.7 GPa up to 9.2 GPa. Six peaks centered at 194.7 cm^{-1} (R1), 208.1 cm^{-1} (R2), 260.5 cm^{-1} (R3), 275.1 cm^{-1} (R4), 268.3 cm^{-1} (R5, at pressures larger than 2.9 GPa) and 221.8 cm^{-1} (R6, in 2.4-2.6 GPa pressure range) can be observed. These peaks disappear above ∼2.0 GPa (R1), 2.4 GPa (R3 and R4) and 2.6 GPa (R2 and R6). Above 2.6 GPa, only the R5 peak is measured until ∼5.2 GPa. Such findings are closely related to variations in the cross-section of the tube [22, 39, 51–53]. As it will be discussed later, these peaks can be assigned to the beginning (2.0 GPa) and the end (5.2 GPa) of the radial collapse process of these tubes. The RBLMs fitting is carried out in a similar way than our previous works on DWCNTs and TWCNTs [17, 53] using Lorentzian profiles (Fig. 4a) for the RBLMs modes. The corresponding Raman frequencies are plotted as function of pressure in Fig. 4b. Except for the R6 peak, which does not present enough experimental points to carry out a reliable fitting, we observe that the RBLM frequencies increase linearly with pressure, in agreement with other results in the literature. [17, 31].

Previous studies have shown that the pressure coefficient of RBLMs ($\partial\omega/\partial P$) are smaller for the inner dominant modes than for the outer dominant ones in double- and triple-wall CNTs due to chemical screening effect and structural support [17, 31, 53]. By comparing $\partial\omega/\partial P$ with values found in the literature [17, 31] (see Table 1), we observe that our samples present lower values, indicating that our RBLMs are dominated by the innermost tubes. The observation of inner/outer tubes dominated RBLMs in the different studies

Table 1: RBLM frequencies (ω_0) and pressure coefficient ($\partial\omega/\partial P$) of double-wall CNTs for different pressure-transmitting media: NaCl (Ref. [17] and our results), paraffin oil (Ref. [17]) and 4:1 methanol-ethanol (Ref. [31]).

Feature	ω_0 (cm^{-1})	$\partial\omega/\partial P$ (cm^{-1}/GPa)	Origin tube
NaCl (this work)			
R1	186.6	1.4±0.2	inner
R2	202.2	2.3±0.7	inner
R3	260.1	1.2±0.7	inner
R4	274.2	2.2±0.8	inner
R5	263.4	2.0±0.5	inner
NaCl (Ref. [17])			
R1	160.3	7.0±0.3	outer
R2	172.4	6.7±0.3	outer
R5	250.1	1.4±0.1	inner
R6	260.8	2.1±0.3	inner
R7	270.1	1.4±0.2	inner
Paraffin oil (Ref. [17])			
R1	162.6	4.8±0.4	outer
R2	175.1	4.1±0.2	outer
R5	249.5	1.8±0.1	inner
R6	259.8	2.3±0.2	inner
R7	267.6	1.6±0.2	inner
4:1 methanol-ethanol (Ref. [31])			
R1	175	5.8	outer
R2	186	5.8	outer
R4	323	1.5	inner
R5	384	1.1	inner

shown in Tab. 1 is dependent on the particular diameter and chirality distribution in each sample as well as on the excitation wavelength used in the Raman study. For pressures beyond 2.6 GPa only one peak (R5) is observed in the energy domain of R3 and R4 whereas a single very broad feature replaces R1 and R2. It is difficult to make a clear assignment of these new peaks. We can recall here that modeling of the projected phonon-DOS at the RBLMs energy domain in DWCNT during radial section deformation shows a clear broadening [38].

Figure 5a shows the evolution of the G-band as a function of pressure. In general, we observe that the peaks broaden and their intensity decreases with increasing pressure. The same trend was observed in previous works [17, 31]. In Fig. 5b we show the evolution of the G-band frequencies with pressure. As suggested in Ref. [17, 31], we fitted the G-band profile with four Lorentzian peaks. For double-wall CNTs, it was proposed that the two highest frequency components can be assigned to G^+ modes, and more precisely that the highest frequency is due to the outer tubes while the next highest is related to the inner tubes [17, 31]. The two remaining lower frequency components are then assigned as G^- peaks. We recognize that the pressure evolution of the weak and broader G_i^- is not obvious. Nevertheless, we observe a strong consistency on its pressure evolution both of its position and width with the other 3 G-band components. We may note that the FWHM of the four G-band components become broader for the lowest energy ones and that the G_i^- is particularly broad (see supplementary information). All

the FWHM of the G-components increase with pressure up to 3-4 GPa. From this value there is a clear reduction of the FWHM with pressure. This will be discussed later.

Experimental and theoretical studies have shown that the change of sign of the pressure derivative of the G-band marks the beginning of the radial collapse of the tube [14, 15, 17, 54]. The loss of RBM resonances is attributed in literature either to a change in resonance conditions [22, 39, 52, 53] or to a drastic cross-section deformation, or even to the collapse of the CNT [14, 39, 51]. We observed a change of sign of the pressure derivatives for all G-band components of our double-wall CNTs at $\sim$1 GPa. It is not possible to clearly establish if there is a corresponding change in the RBLM peaks. At $\sim$2 GPa the G-band peaks energy pressure slope starts to evolve to become positive again associated to the loss of the R1, R2, R3, R4 and R6 RBLM peaks. These two simultaneous observations can be assigned to the onset of the collapse in these CNTs. Furthermore, the four G-band components tend to evolve towards a monotonic behavior that is reached at about $\sim$5 GPa, which can be then explained by a graphite-like response (see Fig. 5b) in the collapsed form. This pressure of $\sim$5 GPa should then correspond to the end of the collapse process. Moreover, as pointed out before, the R5 peak also disappears at $\sim$5.2 GPa. Similar results for the RBLMs have been obtained by Shujie *et al* [39] for the collapse of the outer tubes with different diameters. Our observation of a maximum value of FWHM of the G-band components at 3-4 GPa, would then correspond with the highest degree of disorder due

to mixing between pristine and collapsed geometries.

Aguiar *et al.* [17] suggested different collapse pressures for inner and outer tubes in double-wall CNTs proposing a cascade-type collapse process. However, from the G-band evolution, our results show both tubes collapsing at about the same pressure. We can understand this difference by reminding that we have assigned the change of sign of the slope of the G-band to the onset of the collapse and the graphitic behavior to the fully collapsed geometry, while the change of sign was previously assumed as marking the full collapse of the tube.

Finally, in Fig. 6 we compare experimental collapse pressures for double-wall CNTs with the theoretical curves obtained by fitting our DFTB results. In the graph is represented the normalized collapse pressure as function of the inner tube diameter. It is included in continuous line the modified Lévy-Carrier law following Eq.1 as well as the linear variation found from the high diameter deviations shown in Fig. 1. The continuous lines represent then our prediction for the collapse pressure dependence on tube diameter. The collapse pressures obtained experimentally in our work and in Refs. [17] and [39] are also included in the graph. The large incertitudes in the experimental points at low diameters arise both from incertitudes in the collapse pressure and on the tube diameter determination. We should remind that the experiment of Ref. [39] was performed on double-wall CNTs solubilised in sodium-cholate water solution (not bundles) which also worked as the pressure-transmitting medium. It is also important to remark that

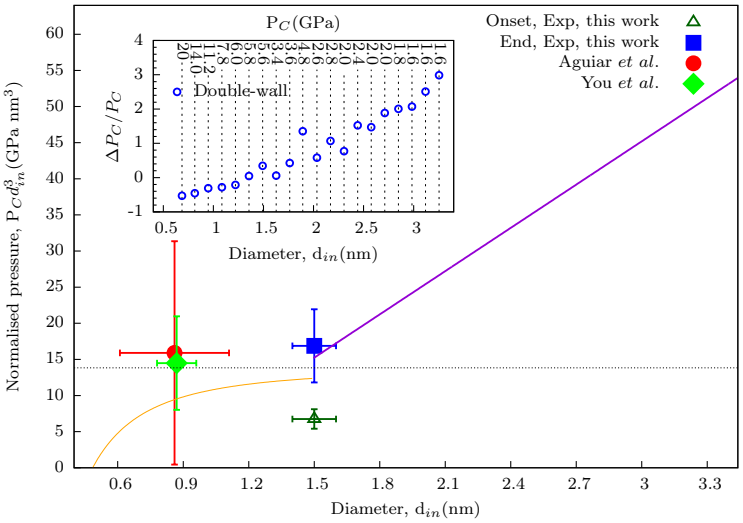

Figure 6: DWCNT normalized collapse pressure as a function of the inner diameter. Symbols correspond to our experimental data as well as data from A. Aguiar et al. (Ref. [17]) and S. You et al. (Ref. [39]). The solid curved line is a fit of Eq. 1 (α =13.8 GPa nm^3 and β =0.48 nm) and the solid straight line is the linear fit shown in Fig. 1 calculated in this work. The dashed black line corresponds to the continuum mechanics prediction by taking $\beta = 0$. The solid lines from our DFTB calculations correspond to the end of collapse. The onset of collapse obtained from our experiments is also shown for comparison. The inset shows the normalized relative difference in collapse pressure between the calculated DFTB data and the continuum medium model as function of the inner tube diameter (normalized by the Lvy-Carrier collapse pressure). Our calculated collapse pressure in GPa is shown also in the top horizontal axis of the inset.

open single-wall CNTs having diameters as small as 0.55 nm become filled with water in surfactant-water solutions [55]. Also, a study on empty and water-filled single-wall CNTs showed that the collapse pressure increases significantly upon water filling [14]. Therefore, the higher values of the collapse pressure in Fig. 6 of Ref. [39] could be explained by an unintentional filling of the CNTs. At such high pressures, the non-hydrostaticity of the pressure transmitting medium can also have an effect in the values of the collapse pressures, making more difficult the comparison between experimental and calculated values. In all cases, Fig. 6 makes clear that the present precision on the study of the collapse of DWCNT does not allow to discriminate between the predictions of continuum mechanics (horizontal line in Fig. 6) and the corrections introduced either by atomic discretization or intertube interactions. The inset in Fig. 6 shows the difference in collapse pressure between the continuum mechanics model and our calculations normalized with respect to the continuum mechanics values. These differences clearly indicate that the expected deviations can be very important for DWCNT with tube diameters beyond $\sim$ 2 nm allowing to discriminate between models. The study of samples with selected diameters or chilarities - in a similar way as was done in SWCNT [30] - or the study of well characterized individual tubes appears then as the most promising strategy for such discrimination. We underline that our predictions show an enhancement of tube stability through bundling with respect to the continuum mechanics predictions which can be more than 3-fold for the larger investigated tubes.

In Fig. 6 we have also included the pressure corresponding to the onset of the collapse in our Raman experiment (triangle symbol). The recent analytic solution for the collapse of the simple elastic ring under pressure [56, 57] showed a progressive process starting at P_c and finishing at 1.5 P_c. Our experimental results for double-wall carbon nanotubes having inner and outer diameters averaging 1.5 nm and 2.0 nm, respectively show a progressive collapse extending between 2 and 5 GPa which corresponds to an extension up to 2.5 P_c, i.e., significantly more important than the predictions of continuum mechanics. This difference could be attributed to the sequential process of the pressure induced collapse in double-wall CNT [17] related to the non continuum nature of their structure.

4. Conclusions

We performed a combined experimental and theoretical study on the collapse of few-wall carbon nanotubes bundles under pressure. Calculations show that the collapse pressure does not follow a simple $1/d_{in}^3$ law, corresponding to the Lévy-Carrier continuous medium prediction. Deviations of distinct origin and opposite directions have been found both in the low diameter regime due to atomic discretization effects [30] (collapse pressure reduction) and for diameters higher than $\sim$ 1.5 nm attributed to inter-tube interactions (collapse pressure enhancement). The collapse process is, however, more complex for the case of few-wall tubes (with respect to their single-wall counterparts), as the outer tube cross-section can be modified at

lower pressures, leading then to an inhomogeneous compression of the inner tubes. This can, in turn, reduce the mechanical stability of the few-walled tube. This effect seems to be particularly important when the distance between inner and outer walls increases. Experimentally we have determined the onset and end of collapse of DWCNT having 1.5 nm internal diameter and graphite-like distance between the tubes. Our experimental values of the collapse pressure as well as others find in the literature for lower tube diameters do agree with our findings but can also be compatible with a continuum mechanics model. Experiments in DWCNT samples with well characterized diameters and not having penetration from the pressure transmitting medium (closed tubes) will be needed to discriminate between our predicted values of collapse pressure and the predictions of continuum mechanics. All these results appear of particular importance in view of an engineering of composite materials or devices through strain engineering.

Acknowledgments

Brazilian authors acknowledge funding from CNPq (grant 307317/2010-2, INCT NanoBioSimes) and Central Analítica-UFC/CT-INFRA-FINEP/Pró-Equipamentos-CAPES/CNPq-SisNano-MCTI (grant 402284/2013-5). R. S. Alencar is also in debt to Coordenação de Aperfeiçoamento de Pessoal de Nível Superior (CAPES) under the grant No. 99999.004227/2014-00 for financial support. Alexander Soldatov (University of Lulea, Sweden) is warmly acknowledged for discussions on the RBM Raman spectra interpretation at

the collapse region.

[1] A. Jorio, M. S. Dresselhaus, G. Dresselhaus, Carbon nanotubes: advanced topics in the synthesis, structure, properties and applications, Springer, 2008.

[2] J. P. Lu, Elastic properties of carbon nanotubes and nanoropes, Phys. Rev. Lett. 79 (1997) 1297–1300. doi:10.1103/PhysRevLett.79.1297.

[3] A. Krishnan, E. Dujardin, T. W. Ebbesen, P. N. Yianilos, M. M. J. Treacy, Young's modulus of single-walled nanotubes, Phys. Rev. B 58 (1998) 14013–14019. doi:10.1103/PhysRevB.58.14013.

[4] A. Sood, P. Teresdesai, D. Muthu, R. Sen, A. Govindaraj, C. Rao, Pressure behaviour of single wall carbon nanotube bundles and fullerenes: A Raman study, Phys. Status Solidi B 215 (1) (1999) 393–401, International Conference on Solid State Spectroscopy - (ICSSS), Schwabisch Gmund, Germany, Sep 05-07, 1999. doi:10.1002/(SICI)1521-3951(199909)215:1¡393::AID-PSSB393¿3.0.CO;2-8.

[5] U. Venkateswaran, Squeezing carbon nanotubes, Phys. Status Solidi B 241 (14) (2004) 3345–3351, 11th International Conference on High-Pressure Semiconductor Physics (HPSP-11), Berkeley, CA, AUG 02-05, 2004. doi:10.1002/pssb.200405236.

[6] J. A. Elliott, J. K. W. Sandler, A. H. Windle, R. J. Young, M. S. P.

Shaffer, Collapse of single-wall carbon nanotubes is diameter dependent, Phys. Rev. Lett. 92 (2004) 095501. doi:10.1103/PhysRevLett.92.095501.

[7] C. Caillier, A. Ayari, V. Gouttenoire, J.-M. Benoit, V. Jourdain, M. Picher, M. Paillet, S. Le Floch, S. T. Purcell, J.-L. Sauvajol, A. San Miguel, An Individual Carbon Nanotube Transistor Tuned by High Pressure, Adv. Funct. Mater. 20 (19) (2010) 3330–3335. doi:10.1002/adfm.201000398.

[8] M. Popov, M. Kyotani, R. J. Nemanich, Y. Koga, Superhard phase composed of single-wall carbon nanotubes, Phys. Rev. B 65 (2002) 033408. doi:10.1103/PhysRevB.65.033408.

[9] V. Perebeinos, J. Tersoff, Carbon nanotube deformation and collapse under metal contacts, Nano Lett. 14 (8) (2014) 4376–4380, pMID: 25014612. arXiv:http://dx.doi.org/10.1021/nl5012646, doi:10.1021/nl5012646.

[10] M. Lévy, Mémoire sur un nouveau cas intégrable du probleme de l'élastique et l'une de ses applications, Journal de Mathématiques Pures et Appliquées 3 (1884) 5–42.

[11] A. P. Carman, Resistance of tubes to collapse, Phys. Rev. XXI (1905) 381–387.

[12] G. F. Carrier, On the buckling of elastic rings., J. Math. Phys. 26.

[13] T. F. Cerqueira, S. Botti, A. San-Miguel, M. A. Marques, Density-functional tight-binding study of the collapse of carbon nanotubes under hydrostatic pressure, Carbon 69 (0) (2014) 355–360.

[14] A. C. Torres-Dias, S. Cambré, W. Wenseleers, D. Machon, A. San-Miguel, Chirality-dependent mechanical response of empty and water-filled single-wall carbon nanotubes at high pressure, Carbon (2015) 442–541doi:10.1016/j.carbon.2015.08.032.

[15] C. Caillier, D. Machon, A. San-Miguel, R. Arenal, G. Montagnac, H. Cardon, M. Kalbac, M. Zukalova, L. Kavan, Probing high-pressure properties of single-wall carbon nanotubes through fullerene encapsulation, Phys. Rev. B 77 (12) (2008) 125418. doi:10.1103/PhysRevB.77.125418.

[16] L. Alvarez, J.-L. Bantignies, R. Le Parc, R. Aznar, J.-L. Sauvajol, A. Merlen, D. Machon, A. San Miguel, High-pressure behavior of polyiodides confined into single-walled carbon nanotubes: A raman study, Phys. Rev. B 82 (2010) 205403. doi:10.1103/PhysRevB.82.205403.

[17] A. L. Aguiar, E. B. Barros, R. B. Capaz, A. G. Souza Filho, P. T. C. Freire, J. Mendes Filho, D. Machon, C. Caillier, Y. A. Kim, H. Muramatsu, M. Endo, A. San-Miguel, Pressure-induced collapse in double-walled carbon nanotubes: Chemical and mechanical screening effects, J. Phys. Chem. C 115 (13) (2011) 5378–5384. doi:10.1021/jp110675e.

[18] B. Anis, K. Haubner, F. Börrnert, L. Dunsch, M. H. Rümmeli, C. A. Kuntscher, Stabilization of carbon nanotubes by filling with inner tubes: An optical spectroscopy study on double-walled carbon nanotubes under hydrostatic pressure, Phys. Rev. B 86 (2012) 155454. doi:10.1103/PhysRevB.86.155454.

[19] B. Anis, F. Boerrnert, M. H. Ruemmeli, C. A. Kuntscher, High-Pressure Optical Microspectroscopy Study on Single-Walled Carbon Nanotubes Encapsulating C-60, J. Phys. Chem. C 117 (42) (2013) 21995–22001. doi:10.1021/jp405639t.

[20] W. Cui, T. F. T. Cerqueira, S. Botti, M. A. L. Marques, A. San-Miguel, Nanostructured water and carbon dioxide inside collapsing carbon nanotubes at high pressure, Phys. Chem. Chem. Phys. (2016) – doi:10.1039/C6CP03263J.

[21] A. J. Ghandour, I. F. Crowe, J. E. Proctor, Y. W. Sun, M. P. Halsall, I. Hernandez, A. Sapelkin, D. J. Dunstan, Pressure coefficients of raman modes of carbon nanotubes resolved by chirality: Environmental effect on graphene sheet, Phys. Rev. B 87 (2013) 085416.

[22] A. Merlen, P. Toulemonde, N. Bendiab, A. Aouizerat, J. Sauvajol, G. Montagnac, H. Cardon, P. Petit, A. San Miguel, Raman spectroscopy of open-ended single wall carbon nanotubes under pressure: effect of the pressure transmitting medium, Phys. Status Solidi B 243 (3) (2006) 690–699.

[23] P. Puech, E. Flahaut, A. Sapelkin, H. Hubel, D. J. Dunstan, G. Landa, W. S. Bacsa, Nanoscale pressure effects in individual double-wall carbon nanotubes, Phys. Rev. B 73 (2006) 233408. doi:10.1103/PhysRevB.73.233408.

[24] F. Balima, S. L. Floch, C. Adessi, T. F. Cerqueira, N. Blanchard, R. Arenal, A. Brlet, M. A. Marques, S. Botti, A. San-Miguel, Radial collapse of carbon nanotubes for conductivity optimized polymer composites, Carbon 106 (2016) 64 – 73. doi:http://dx.doi.org/10.1016/j.carbon.2016.05.004.

[25] S. Lebedkin, K. Arnold, O. Kiowski, F. Hennrich, M. M. Kappes, Raman study of individually dispersed single-walled carbon nanotubes under pressure, Phys. Rev. B 73 (2006) 094109. doi:10.1103/PhysRevB.73.094109.

[26] U. D. Venkateswaran, A. M. Rao, E. Richter, M. Menon, A. Rinzler, R. E. Smalley, P. C. Eklund, Probing the single-wall carbon nanotube bundle: Raman scattering under high pressure, Phys. Rev. B 59 (1999) 10928–10934. doi:10.1103/PhysRevB.59.10928.

[27] A. Merlen, N. Bendiab, P. Toulemonde, A. Aouizerat, A. San Miguel, J. L. Sauvajol, G. Montagnac, H. Cardon, P. Petit, Resonant raman spectroscopy of single-wall carbon nanotubes under pressure, Phys. Rev. B 72 (2005) 035409. doi:10.1103/PhysRevB.72.035409.

[28] D. J. Dunstan, A. J. Ghandour, High-pressure studies of carbon nanotubes, High Pressure Res. 29 (4) (2009) 548–553, 47th Meeting of the European-High-Pressure-Research-Group (EHPRG 47), Univ Pierre & Marie Curie, Cordeliers Campus, Paris, France, Sep 06-11, 2009. doi:10.1080/08957950903438473.

[29] A. J. Ghandour, D. J. Dunstan, A. Sapelkin, I. Hernandez, M. P. Halsall, I. F. Crowe, Effect of water on resonant raman spectroscopy of closed single-walled carbon nanotubes, Phys. Status Solidi B 248 (11) (2011) 2548–2551. doi:10.1002/pssb.201100074.

[30] A. C. Torres-Dias, T. F. Cerqueira, W. Cui, M. A. Marques, S. Botti, D. Machon, M. A. Hartmann, Y. Sun, D. J. Dunstan, A. San-Miguel, From mesoscale to nanoscale mechanics in single-wall carbon nanotubes., Carbon (2017) – doi:https://doi.org/10.1016/j.carbon.2017.07.036.

[31] J. Arvanitidis, D. Christofilos, K. Papagelis, K. S. Andrikopoulos, T. Takenobu, Y. Iwasa, H. Kataura, S. Ves, G. A. Kourouklis, Pressure screening in the interior of primary shells in double-wall carbon nanotubes, Phys. Rev. B 71 (2005) 125404. doi:10.1103/PhysRevB.71.125404.

[32] P. Puech, H. Hubel, D. J. Dunstan, R. R. Bacsa, C. Laurent, W. S. Bacsa, Discontinuous tangential stress in double wall carbon nanotubes, Phys. Rev. Lett. 93 (2004) 095506. doi:10.1103/PhysRevLett.93.095506.

[33] X. Ye, D. Y. Sun, X. G. Gong, Pressure-induced structural transition of double-walled carbon nanotubes, Phys. Rev. B 72 (2005) 035454. doi:10.1103/PhysRevB.72.035454.

[34] X. Yang, G. Wu, J. Dong, Structural transformations of double-walled carbon nanotube bundle under hydrostatic pressure, Appl. Phys. Lett. 89 (11) (2006) –. doi:10.1063/1.2266529.

[35] P. Puech, H. Hubel, D. J. Dunstan, A. Bassil, R. Bacsa, A. Peigney, E. Flahaut, C. Laurent, W. S. Bacsa, Light scattering of double wall carbon nanotubes under hydrostatic pressure: pressure effects on the internal and external tubes, Phys. Status Solidi B 241 (14) (2004) 3360–3366. doi:10.1002/pssb.200405227.

[36] E. del Corro, J. Gonzlez, M. Taravillo, E. Flahaut, V. G. Baonza, Raman spectra of double-wall carbon nanotubes under extreme uniaxial stress, Nano Lett. 8 (8) (2008) 2215–2218, pMID: 18593203. doi:10.1021/nl080760o.

[37] M. Mases, V. V. Milyavskiy, J. Waldbock, M. Dossot, X. Devaux, E. McRae, A. V. Soldatov, The effect of shock wave compression on double wall carbon nanotubes, Phys. Status Solidi B 249 (12).

[38] A. L. Aguiar, R. B. Capaz, A. G. Souza Filho, A. San-Miguel, Structural and phonon properties of bundled single- and double-wall carbon nan-

otubes under pressure, J. Phys. Chem. C 116 (42) (2012) 22637–22645. doi:10.1021/jp3093176.

[39] S. You, M. Mases, I. Dobryden, A. A. Green, M. C. Hersam, A. V. Soldatov, Probing structural stability of double-walled carbon nanotubes at high non-hydrostatic pressure by raman spectroscopy, High Pressure Res. 31 (1) (2011) 186–190. doi:10.1080/08957959.2011.562897.

[40] D. Porezag, T. Frauenheim, T. Köhler, G. Seifert, R. Kaschner, Construction of tight-binding-like potentials on the basis of density-functional theory: Application to carbon, Phys. Rev. B 51 (1995) 12947–12957.

[41] G. Seifert, D. Porezag, T. Frauenheim, Calculations of molecules, clusters, and solids with a simplified lcao-dft-lda scheme, Int. J. Quantum Chem. 58 (2) (1996) 185–192.

[42] J. Frenzel, A. F. Oliveira, N. Jardillier, T. Heine, G. Seifert, Semi-relativistic, self-consistent charge slater-koster tables for density-functional based tight-binding (dftb) for materials science simulations. (2004).

[43] G. Zheng, S. Irle, K. Morokuma, Performance of the dftb method in comparison to dft and semiempirical methods for geometries and energies of c20-c60 fullerene isomers, Chem. Phys. Lett. 412 (1 - 3) (2005) 210 – 216. doi:10.1016/j.cplett.2005.06.105.

[44] S. Malola, H. Häkkinen, P. Koskinen, Raman spectra of single-walled carbon nanotubes with vacancies, Phys. Rev. B 77 (2008) 155412. doi:10.1103/PhysRevB.77.155412.

[45] S. Botti, M. Amsler, J. A. Flores-Livas, P. Ceria, S. Goedecker, M. A. Marques, Carbon structures and defect planes in diamond at high pressure, Phys. Rev. B 88 (1) (2013) 014102.

[46] Z. Peralta-Inga, S. Boyd, J. S. Murray, C. J. O'Connor, P. Politzer, Density functional tight-binding studies of carbon nanotube structures, Struct. Chem. 14 (5) (2003) 431–443.

[47] E. Flahaut, C. Laurent, A. Peigney, Catalytic {CVD} synthesis of double and triple-walled carbon nanotubes by the control of the catalyst preparation, Carbon 43 (2) (2005) 375–383. doi:10.1016/j.carbon.2004.09.021.

[48] H. Mao, J. Xu, P. Bell, Calibration of the ruby pressure gauge to 800-kbar under quasi-hydrostatic conditions, J. Geophys. Res. 91 (B5) (1986) 4673–4676. doi:10.1029/JB091iB05p04673.

[49] J. Zang, A. Treibergs, Y. Han, F. Liu, Geometric constant defining shape transitions of carbon nanotubes under pressure, Phys. Rev. Lett. 92 (2004) 105501. doi:10.1103/PhysRevLett.92.105501.

[50] S. Rols, I. N. Goncharenko, R. Almairac, J. L. Sauvajol, I. Mirebeau,

Polygonization of single-wall carbon nanotube bundles under high pressure, Phys. Rev. B 64 (2001) 153401. doi:10.1103/PhysRevB.64.153401.

[51] M. J. Peters, L. E. McNeil, J. P. Lu, D. Kahn, Structural phase transition in carbon nanotube bundles under pressure, Phys. Rev. B 61 (2000) 5939–5944. doi:10.1103/PhysRevB.61.5939.

[52] A. J. Ghandour, D. J. Dunstan, A. Sapelkin, J. E. Proctor, M. P. Halsall, High-pressure raman response of single-walled carbon nanotubes: Effect of the excitation laser energy, Phys. Rev. B 78 (2008) 125420. doi:10.1103/PhysRevB.78.125420.

[53] R. S. Alencar, A. L. Aguiar, A. R. Paschoal, P. T. C. Freire, Y. A. Kim, H. Muramatsu, M. Endo, H. Terrones, M. Terrones, A. San-Miguel, M. S. Dresselhaus, A. G. Souza Filho, Pressure-Induced Selectivity for Probing Inner Tubes in Double- and Triple-Walled Carbon Nanotubes: A Resonance Raman Study, J. Phys. Chem. C 118 (15) (2014) 8153–8158. doi:10.1021/jp4126045.

[54] M. Yao, Z. Wang, B. Liu, Y. Zou, S. Yu, W. Lin, Y. Hou, S. Pan, M. Jin, B. Zou, T. Cui, G. Zou, B. Sundqvist, Raman signature to identify the structural transition of single-wall carbon nanotubes under high pressure, Phys. Rev. B 78 (20) (2008) 205411. doi:10.1103/PhysRevB.78.205411.

[55] S. Cambré, B. Schoeters, S. Luyckx, E. Goovaerts, W. Wenseleers, Ex-

perimental observation of single-file water filling of thin single-wall carbon nanotubes down to chiral index (5,3), Phys. Rev. Lett. 104 (20) (2010) 207401. doi:10.1103/PhysRevLett.104.207401.

[56] P. Djondjorov, V. Vassilev, I. Mladenov, Analytic description and explicit parametrisation of the equilibrium shapes of elastic rings and tubes under uniform hydrostatic pressure, Int. J. Mech. Sci 53 (2011) 355–364.

[57] V. Vassilev, P. Djondjorov, I. Mladenov, Comment on "shape transition of unstrained flattest single-walled carbon nanotubes under pressure" [j. appl. phys. 115, 044512 (2014)], J. Appl. Phys. 117 (2015) 196101.